Est. 1984

ORIENTAL JOURNAL OF CHEMISTRY
An International Open Access, Peer Reviewed Research Journal

www.orientjchem.org

ISSN: 0970-020 X
CODEN: OJCHEG
2023, Vol. 39, No.(4):
Pg. 890-895

Dual Mode Photoluminescence Studies of Polyol-mediated Ho^{3+} Doped $CePO_4$

SIRISHA BANDI[1,2]*, PHANI RAJA KANUPARTHY[1]* and VENKATA NAGENDRA KUMAR PUTTA[1]

[1]Department of Chemistry, GITAM deemed to be University, Rudraram, Hyderabad-502329, India.
[2]B V Raju Institute of Technology, Narsapur,502313, Telangana, India.
*Corresponding author E-mail:bandisireesha@gmail.com

http://dx.doi.org/10.13005/ojc/390409

(Received: June 21, 2023; Accepted: August 14, 2023)

ABSTRACT

In this work, $CePO_4$:Ho^{3+} nanomaterials are prepared by a productive polyol method which shows the dual mode of behavior in Photoluminescence. The up-conversion spectra at 980nm excitation display a sharp brilliant peak at ~520nm- ~550nm, ~630nm, -670nm resulting in the ($^5F_4$, $^5S_2 \rightarrow {}^5I_8$) and ($^5F_5 \rightarrow {}^5I_8$) of Ho^{3+} ions, and it is also found that the sample radiates green and red colors. The down-conversion peaks show maximum absorption at 300nm which exhibit peaks at ~450nm, ~520nm- ~550nm, and 630nm- ~670nm respectively. The rare earth ions doped nanomaterials show up-conversion radiation and down-conversion radiation. This type of energetic work has an extensive range of applications, including lasers, metal ion sensors, bio-imaging, temperature and stress sensors, radiation damage sensors, and defense and cyber security.

Keywords: Down-conversion, Up-conversion, Polyol method, Photoluminescence, Cerium ion, Holmium ion.

INTRODUCTION

With the rapid development of rare earth minerals, they are currently referred to as inorganic vitamins. These rare earth-doped nano-phosphors are a distinct group of light-emitting materials whose spectrum properties are determined by the 4f level spacing of a certain lanthanide ion. This shows a range of narrow emissions from visible to near-infrared, and there are numerous uses for rare earth-doped phosphors. They are high-resolution display systems, electronic devices, security, and medical diagnostics, among other things.[1–6] new research on these phosphors. Bio-imaging and energy are the two main areas that it covers. The up-conversion (UC) and down-conversion (DC) properties of lanthanide nano-particles are used in collectors-imaging research because they are projected to improve bio-imaging from multiple aspects, including penetration depth, insignificant auto-fluorescence, and lesser scattering.[3] In this present work ($CePO_4$:Ho^{3+}) here cerium phosphate is doped with holmium which gives tremendous applications and the emission peaks of Ho^{3+} give upconversion (UC) and down-conversion (DC). Because of various restrictions imposed by its

nature, such as the laser's small spot size (1-2mm diameter) and the necessity for suitable filters and collimators[7-8], literature research using NIR light excitation is few. The NIR light's deep penetration, which enables it to detect materials with a few cm thicknesses, therefore, has significant benefits over UV light excitation if the abovementioned limits are resolved. Due to its superior physical and chemical characteristics, cerium would be a rare earth element that is frequently employed. Due to their appealing catalytic activities and electrical conductivity characteristics, Ce-based nanomaterials have grown to be very important for electrochemical biosensors.[9–11] The preparation of Ce-based nanomaterials has a substantial impact on their electrochemical application-related properties. In this method of doping, we can observe the phase transfer of hexagonal to monoclinic can be observed from most of the literature and the given data.

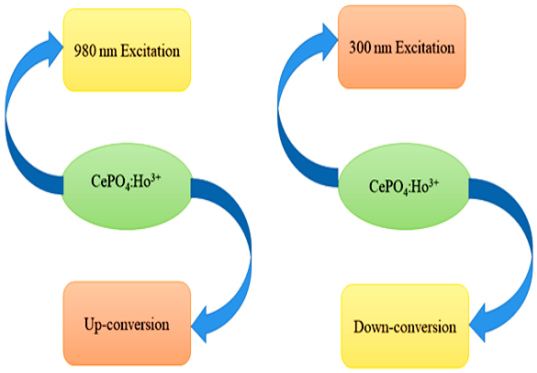

Fig. 1. A Graphical representation of properties studies of $CePO_4:Ho^{3+}$ at 980nm and 300nm excitations

MATERIALS AND METHODS

Chemicals required and process of synthesis

Chemicals required

Reagents of the highest purity Sigma-Aldrichwere utilized as reactants without additional purification. Cerium(III) acetate Hydrated($Ce(ac)_3$). XH_2O, Ammonium dihydrogen phosphate $(NH_4)_2HPO_4$, Holmium (III) acetate hydrate ($HO(ac)_3$).XH_2O, dil HCl, Ethylene glycol, dil NaOH, and deionized water were used as precursors.

Synthesis of $CePO_4:Ho^{3+}$ Nanoparticles

We prepared the sample via the polyol technique.

Samples prepared were

The polyol method was used to create $CePO_4:Ho^{3+}$ luminescent nanoparticles with varying Ho^{3+} concentrations (1%, 3%, 5%, and 7% atomic percent). The procedure is described as follows:

Step I. Starting Materials: 991.3 mg of $(CH_3CO_2)_3Ce.xH_2O$ (cerium acetate hydrate), 8.7 mg of $(CH_3CO_2)_3Ho.xH_2O$ (holmium acetate hydrate), 5 mL of concentrated HCl (hydrochloric acid), 10 mL of deionized water, 298.2 mg of $(NH_4)_2HPO_4$ (ammonium phosphate), 2.64 g of NaOH (sodium hydroxide), 20 mL of EG (ethylene glycol).

Step II. Holmium and Cerium Acetate Dissolution: In 5 cc of concentrated HCl, the cerium and holmium acetate hydrates are heated until they are completely dissolved. As a result, a crystal-clear solution containing the metal ions is created.

Step III. Elimination of Extra HCl: By alternative addition of 10 mL of deionized water to the solution by repeating this process 5 times excess of HCl is eliminated. Throughout this procedure, the solution is heated to 80°C.

Step-IV. The $(NH_4)_2HPO_4$ and NaOH solution are prepared: In 10 mL of deionized water, 298.2 mg of $(NH_4)_2HPO_4$ and 2.64 g of NaOH are dissolved. This results in a translucent $(NH_4)_2HPO_4$ and NaOH solution.

Step-V. Addition of $(NH_4)_2HPO_4$ Solution: Until the $(NH_4)_2HPO_4$ solution turns translucent, the NaOH solution is gradually added drop by drop. The solution acquires a little yellow hue as a result of this reaction.

Step-VI. Development of Precipitate: In a 100 mL round-bottom flask, the evaporated metal ion solution from step 3 is transferred. The flask is filled with 20 mL of EG. The mixture is refluxed at 80°C for 10 minutes. The $(NH_4)_2HPO_4$ solution is then poured into the flask drop by drop. Over two hours of heating at 120°C, the solution progressively becomes white. During this procedure, a white precipitate is created in the solution.

Step-VII. Cleaning and Gathering: Ten mL of acetone is used to rinse the precipitate twice. It is then collected as a dry powder after being dried using an infrared (IR) light. To separate and gather the nanoparticles, centrifugation is carried out at 5000 rpm for 5 minutes.

Step-VIII. Annealing: The same method is used to create $CePO_4$ nanoparticles doped with different amounts of Ho^{3+} (3%, 5%, and 7% atomic percent). All of the synthesized samples are subjected to a 4 h annealing process at 900°C to improve their crystallinity and optical characteristics.

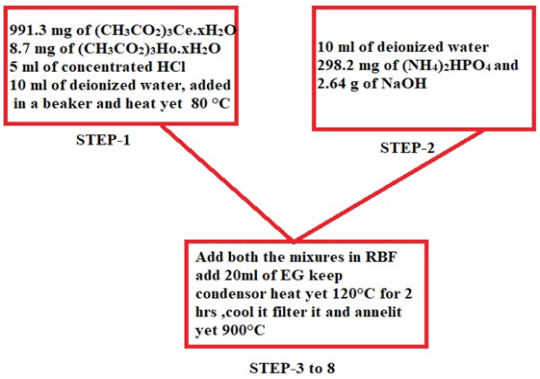

Fig. 1.1. Schematic representation of Synthesis of $CePO_4$:Ho^{3+} Nanoparticles

RESULTS AND DISCUSSION

Instrumentation

For all the prepared samples these are the below characterization techniques and the instruments are used commonly. The crystalline and regular crystallite sizes of the given samples were checked using angle dispersive X-ray diffraction (source: Rigaku MiniFlex 600 X-ray diffractometer). Using a scanning electron microscope, microstructural characterizations of changes in shape and particle size are carried out. (SEM: QUANTA 200). To examine the vibrational structure of the generated materials, FTIR spectroscopy (Bomem MB 102 spectrophotometer) was used. UC emission was measured using a monochromator (iHR320, Horiba Jobin Yvon) fitted with a photomultiplier tube. Using a diode laser, 980 nm radiation was used to stimulate the samples (2W, power continuous mode, adjustable). In up-conversion studies, photoluminescence excitation (PLE) is used to examine the emission spectra of different samples are examined $CePO_4$:Ho^{3+}

X-ray diffraction studies

The XRD pattern of $CePO_4$:1%Ho^{3+} nano phosphor is described in Fig. 2. Here's a summary of the key points: The XRD pattern of $CePO_4$:Ho^{3+} exhibits strong and distinct peaks, indicating a well-defined crystalline structure. The presence of strong peaks and the absence of impurity peaks suggest that the dopants (Ho^{3+} ions) are uniformly dispersed within the $CePO_4$ host lattice. The diffraction pattern matches the characteristic peaks and peak positions expected for the monoclinic phase of $CePO_4$. This indicates that the material has a monoclinic crystal structure. The coordination number (CN) of Ce^{3+} ions in the $CePO_4$ lattice is 8, meaning each Ce^{3+} ion is surrounded by eight oxygen anions. Ho^{3+} ions are substituted at the Ce^{3+} sites of the $CePO_4$ lattice due to their similar ionic radii, resulting in the presence of Ho^{3+} dopants within the material. The coordination of Ce^{3+} to eight oxygen anions results in a hexagonal to monoclinic distortion in the nano phosphor material, consistent with the JCPDS NO.01-083-0652 reference. The reference citation provided 34 likely corresponds to the source where the XRD pattern and its interpretation can be found in more detail.

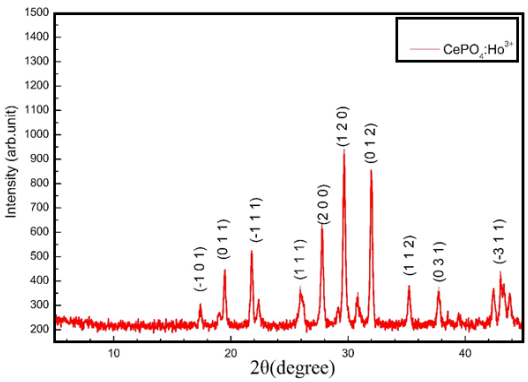

Fig. 2. XRD pattern of $CePO_4$:Ho^{3+} samples respectively

SEM Studies

The SEM picture of $CePO_4$:1%Ho^{3+} nano phosphor material is annealed by applying 900°C which is shown in Fig. 3. It depicts nanoparticles with irregular shapes (a big number of Sponge shapes and a small number of other shapes) (cuboid, cone, rectangle shapes). The normal size of spherical particles is 50 nanometers.

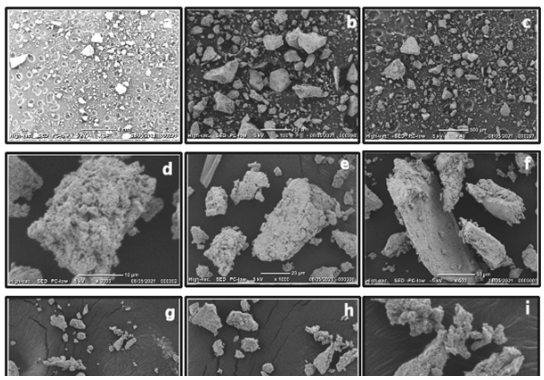

Fig. 3. SEM images of $CePO_4$:Ho^{3+} respectively

FTIR Studies

The vibrational modes and chemical bonds that are present in a material may be learned a lot about FTIR spectroscopy. The $CePO_4$:Ho^{3+} acquired FTIR spectrum exhibits various distinctive peaks that aid in the comprehension of its vibrational structure. FTIR spectrum seen in Fig. 4. has the following full explanation: The $CePO_4$:Ho^{3+} nanomaterial's peak is associated with a particular vibrational mode at a certain wavenumber (cm^{-1}) in the spectrum. Stretching or bending vibrations of the Ce-O, P-O, or Ho-O bonds are examples of potential vibrational modes. The FT-IR spectrum shows another peak at a different wavenumber. A discrete vibrational mode in the nanomaterial is represented by this peak. Each $CePO_4$:Ho^{3+} system's chemical vibrations and bonds determine its exact identification. Phosphate (PO_4) group vibrations or interactions between the dopant ion (Ho^{3+}) and the host lattice are examples of potential assignments. The FTIR spectrum could also show multiple peaks at different wavenumbers. The $CePO_4$:Ho^{3+} nanomaterial's overall vibrational structure is influenced by the individual vibrational modes represented by each peak.we can observe the O-H peak frequently appears in the FTIR spectrum between 3200 and 3600 cm^{-1}, P-O peak at 900–1200 cm^{-1} and Cerium-Oxygen (Ce-O) bands at 800-–1000 cm^{-1} from Figure 4.

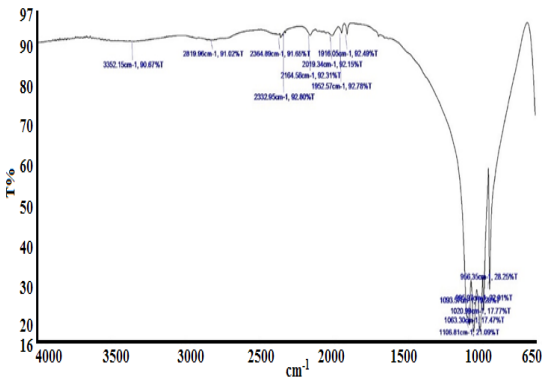

Fig. 4. FTIR of $CePO_4$:Ho^{3+} respectively

Photoluminescence Studies

Photoluminescence of $CePO_4$:Ho^{3+}

Due to its energy levels and electron configurations, the rare-earth element holmium is known for having distinctive optical features. The unique energy level structure of Ho, which has several closely spaced energy levels, is one of the elements that contributes to its dual-mode behavior. The observed up-conversion and down-conversion processes result from interactions between these energy levels and incoming photons of various energies. A defence of the assertion based on Ho's dual-mode behavior is provided here: Holmium has tightly spaced energy levels that make it possible for it to interact with a variety of photon intensities effectively. This implies that transitions between these energy levels can occur as a result of the holmium ions' ability to absorb both lower- and higher-energy photons. Up-Conversion: Holmium ions can boost electrons to higher energy levels when they absorb lower-energy photons. The transitions to even higher energy levels that these excited electrons can make in the future can result in the emission of more powerful photons. This process of "up-conversion" combines many low-energy photons to create a single high-energy photon. Down-conversion: higher-energy photons can cause electrons to be promoted to higher energy levels when they are absorbed by holmium ions. In the process of returning to lower energy levels, these excited electrons can emit a number of lower-energy photons. A single high-energy photon is divided into many low-energy photons during the down-conversion process.Peaks are observed: Holmium's closely spaced energy levels enable effective absorption and emission of photons with a range of energies. As a result, you can see peaks that correspond to both up-conversion and down-conversion processes when examining the emission or absorption spectra of holmium under various circumstances. The energy transitions involved in photon absorption and emission would be represented by these peaks. Due to this dual mode behavior we can observe the similar type of peaks will observe yet Up-conversion & Down-conversion studies from dike book and also we can observe additional peak yet 450nm shows P-O weak charge transfer band. For the given content justification we observe from UC&DC study.

Study

Regarding the nano-phosphor substance from Fig. 5. $CePO_4$:Ho^{3+}'s up-conversion luminescence: A multiphoton optical process called up-conversion luminescence produces high-energy photons while absorbing low-energy ones. It causes photons with energy greater than the excitation source to be emitted as a consequence. The nanophosphor $CePO_4$:Ho^{3+} displays up-conversion fluorescence. Emission of Ho^{3+} Depending on the concentrations of the host and co-dopant, Ho^{3+}

ions in $CePO_4$:Ho^{3+} can produce either green or red emissions[12-16]. $CePO_4$:Ho^{3+} emits in the ranges of 520–550nm (green) and 630–670nm (red), respectively. The Ho^{3+} ion undergoes electronic transitions at $^5S_2$ to $^5I_8$, $^5F_5$ to $^5I_8$, and $^5F_4$ to produce these emissions. Laser ExcitationA laser is used to stimulate $CePO_4$:Ho^{3+} nano-phosphor material yet 980nm. The P-O charge transfer band (CTB) and the $CePO_4$:Ho^{3+} absorption peaks at 450nm are seen in the excitation spectra. The intensity of Up-converted Emission[17-18]: The number of photons included in the up-converted emission bands (n) and the laser input power (P) both affect the up-converted emission intensity (I). The up-converted intensity rises with rising laser power and the number of photons taking part in the process, as shown by the relationship I and Pn. Investigation and optimization. For studies involving up-conversion luminescence, $CePO_4$:1%Ho^{3+} nano-phosphor material, created from 1% Ho^{3+} doped $CePO_4$, is particularly intriguing. When stimulated beyond 980nm, the optimized nano phosphor material displays up-conversion emission spectra with green and red bands[19-20].

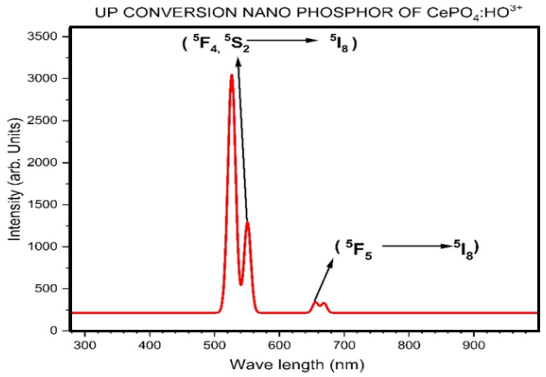

Fig. 5. Emission spectrrum of $CePO_4$:Ho^{3+} (1 at.%Ho^{3+}) excited at 980nm

DC Study

Down-conversion: The main points are summarized as follows:

The Stokes Shift: Following light absorption (Eexc), the procedure involves the emission of lower-energy radiative light (Eem). The emission of light at lower energy compared to the absorbed light is caused by the Stokes shift.[21-22] Emission from Down-Conversion (DC): Fig. 6 displays the $CePO_4$:Ho^{3+} (1% atomic percent Ho) DC emission spectra after UV irradiation at 300nm Excitation, Green (450, 520, and 550nm), red (630-670nm), and other emission bands are seen.[23-24] These bands are connected to electronic transitions of the Ho^{3+} ion ($^5F_4$, $^5S_2$ to $^5I_8$, $^5F_5$$^5I_8$). The emission spectra are measured at various excitation possiblewavelengths (260-300nm). Due to the low absorption cross-section for Ho^{3+} f-f transitions, direct stimulation of Ho^{3+} at 450 results in less intense emission so there is no change observed.The emission peaks linked to Ho^{3+} and the wide emission band 450nm linked to PO_4^{3-} may be seen when stimulated at 300nm.[25] Due to the P-O charge transfer band's (CTB) permitted transition, the absorption cross-section at 300nm is considerable.Ho^{3+}'s radiative rate is increased through energy transfer (ET), Excitation-Dependent Emission.[26] Which occurs via resonance, from PO_4^{3-} to Ho^{3+}.$CePO_4$:Ho^{3+} monitoring is shown in Fig. 6 at 520-550nm emission, with a broad peak seen at 300nm that is due to the P-O CTB transition. Due to Ho3+ emissions, sharp peaks with modest intensities are seen at 450nm, 520 -550nm, and 630-670nm. Ho^{3+} emission peaks are seen when the $CePO_4$ host is stimulated at 300nm with amount of 1% Ho^{3+} doped in. As the Ho^{3+} ion concentration rises above 1%, the luminescence intensity drops.[27] ET Process: The "conn" quenching effect serves as the primary energy source for the energy transfer (ET) process. The luminescence concentration quenching that is seen at greater dopant concentrations is known as the "conn" quenching effect.[28-34]

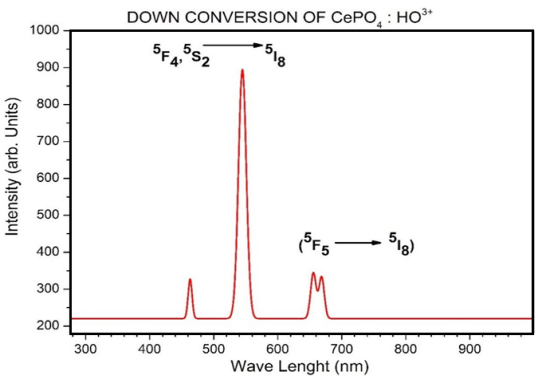

Fig. 6. Excitation spectrum of $CePO_4$: Ho^{3+} (1 at.% Ho) excited at 300nm

CONCLUSION

In conclusion, a polyol-mediated process is successful in producing $CePO_4$:1% Ho^{3+} nanophosphor. After the preparation process, the sample is annealed for 4 h at 900°C to increase crystallinity, eliminate organic components, and

reduce water content. XRD revealed the monoclinic structural phase with space group I41/amd. Yet 980nm excitation, $CePO_4$:0.01Ho^{3+} produces significant up-converted green and red color bands at ~520-550nm ($^5F_4$, $^5S_2 \rightarrow$5 I8), 630-670nm ($^5F_5 \rightarrow {}^5I_8$) of Ho^{3+}. The broad emission band results primarily from ligand to metal CT (P-O CTB). Peaks at 450nm, ~520-550nm ($^5F_4$, $^5S_2 \rightarrow {}^5I_8$), ~630-670nm ($^5F_5 \rightarrow {}^5I_8$), at 300nm excitations of DC be grasped.

ACKNOWLEDGMENT

My heartfelt appreciation goes to GITAM Deemed to be University (Hyderabad) for providing a facility for synthesis.

Conflicts of interest

We have no competing interests that could Influence our research or findings.

REFERENCES

1. Bhonsule, S. U.; Wankhede, S. P.; Moharil, S. V., *AIP Conference Proceedings.*, **2018**, *1953*(1).
2. Perala, R. S.; Singh, B. P.; Putta, V. N. K.; Acharya, R.; Ningthoujam, R. S., *ACS Omega.*, **2021**, *6*(30), 19517-19528.
3. Perala, R. S.; Joshi, R.; Singh, B. P.; Putta, V. N. K.; Acharya, R.; Ningthoujam, R. S., *ACS Omega.*, **2021**, *6*(30), 19471-19483.
4. Szczygieł, I.; Macalik, L.; Radomi ska, E.; Znamierowska, T.; M czka, M.; Godlewska, P.; Hanuza, *J.,Optical Materi.,* **2007**, *29*(9), 1192-1205.
5. Kumar,V.; Wang, G., *Journal of Luminescence.,* **2018**, *199*, 188-193.
6. Parchur, A.K.; Ningthoujam, R.S., *RSC Advances.*, **2012**, *2*(29), 10854-10858.
7. Niu, C.; Li, L.; Li, X.; Lv, Y.; Lang, X., *Optical Materials.*, **2018**, *75*, 68-73.
8. Yu, C.; Yu, M.; Li, C.; Liu, X.; Yang, J.; Yang, P.; & Lin, J., *Journal of Solid State Chemistry.*, **2009**, *182*(2), 339-347.
9. Prorok, K.; Bednarkiewicz, A.; Cichy, B.; Gnach, A.; Misiak, M.; Sobczyk, M.; Strek, W., *Nanoscale.*, **2014**, *6*(3), 1855-1864.
10. AitMellal, O.; Oufni, L.; Messous, M. Y.; Trandafir, M. M.; Chirica, I. M.; Florea, M.; Neau, F., *Journal of Solid State Chemistry.*, **2021**, *301*, 122310.
11. Wang, G.; Peng, Q.; Li, Y., *Accounts of Chemical Research.*, **2021**, *44*(5), 322-332.
12. Kang, X.; Li, C.; Cheng, Z.; Ma, P. A.; Hou, Z.; Lin, J., Wiley Interdisciplinary Reviews: *Nano Medicine and Nano Biotechnology.*, **2014**, *6*(1), 80-101.
13. Kumar, V.; Rani, P.; Singh, D.; Chawla, S., *RSC Advances.*, **2014**, *4*(68), 36101-36105.
14. Suryawanshi, I.; Srinidhi, S.; Singh, S.; Kalia, R.; Kunchala, R. K.; Mudavath, S. L.; Naidu, B.S., *Materials Today Communicat.*, **2021**, *26*, 102144.
15. AitMellal, O.; Oufni, L.; Messous, M.Y.; Trandafir, M. M.; Chirica, I. M.; Florea, M.; Nea u, F., *J. Solid State Chem.,* **2021**, *301*, 122310.
16. Tymin ski, A.; S miechowicz, E.; Martín, I.R.; Grzyb, T., *ACS Applied Nano Materials.,* **2020**, *3*(7), 6541-6551.
17. Lyu,T.; Dorenbos, P., *Journal of Materials Chemistry C.*, **2018**, *6*(2),369-379.
18. Gavrilovi , T.; Periša, J.; Papan, J.; Vukovi , K.; Smits, K.; Jovanovi , D. J.; Drami anin, M. D., *Journal of Luminescence.*, **2018**, *195*, 420-429.
19. Hu, F.; Wei, X.; Qin, Y.;Jiang, S.;Li, X.; Zhou, S.; Yin, M., *Journal of Alloys and Compounds.*, **2016**, *674*, 162-167.
20. Thakur,H.; Singh, B.P.; Kumar, R.; Gathania, A.K.; Singh, S.K.; Singh, R.K., *Materials Chemistry and Physics.*, **2020**, *253*, 123333.
21. Frost, R.; Hales, M.; Martens, W., *J. Thermal Analy. and Calorimetry.*, **2009**, *95*(3), 999-1005.
22. Ren, W.; Tian, G.; Zhou, L.; Yin, W.; Yan, L.; Jin, S.; Zhao, Y., *Nanoscale.*, **2012**, *4*(12), 3754-3760.
23. Yi, Z.; Lu, W.; Qian, C.; Zeng, T.; Yin, L.; Wang, H.; Zeng, S., *Biomateri. Sci.*, **2014**, *2*(10), 1404-1411.
24. Tadge, P.; Yadav, R. S.; Vishwakarma, P. K.; Rai, S. B.; Chen, T. M.; Sapra, S.; Ray, S. *J. Alloys and Compounds.,* **2020**, *821*, 153230.
25. Fang, Y. P.; Xu, A. W.; Song, R. Q.; Zhang, H. X.; You, L. P.; Yu, J. C.; Liu, H. Q., *J. of the Ameri. Chemi. Society.*, **2003**, *125*(51), 16025-16034.
26. Haase,M.; Schäfer, H., *Angewandte Chemie International Edition.*, **2011**, *50*(26), 5808-5829.
27. Sukul, P. P.; Kumar, K., *Methods and Applications in Fluorescence.*, **2016**, *4*(4), 044005.
28. Cesaria,M.; Di Bartolo, B., *Nanomaterials.*, **2019**, *9*(7), 1048.
29. Qu, Z.; Shen, J.; Li, Q.; Xu, F.; Wang, F.; Zhang, X.; Fan, C., *Theranostics.*, **2020**, *10*(6), 2631.
30. Duc-Tin, Q.; Keppler, H., Contributions to *Mineralogy and Petrology.*, **2015**, *169*(1), 1-26.
31. Hudry,D.; Howard,I.A.; Popescu,R.; Gerthsen,D.; Richards, B.S., *Advanced Materials.*, **2019**, *31*(26), 1900623.
32. Yada, M., In Inorganic and Metallic Nano tubular Materials. *Springer, Berlin, Heidelberg.*, **2010**, *48,* 97-115.
33. Runowski, M.; Grzyb, T.; Zep, A.; Krzyczkowska, P.; Gorecka, E.; Giersig, M.; Lis, S., *RSC Advances.*, **2014**, *4*(86), 46305-46312.
34. Bouddouch, A.; Amaterz, E.; Bakiz, B.; Taoufyq, A.; Guinneton, F.; Villain, S.; Benlhachemi, A.,*Optik.*, **2021**, *238*, 166683.